

A role for orbital eccentricity in Earth's seasonal climate

John C. H. Chiang^{1,#} and Anthony J. Broccoli²*

¹ *Department of Geography, University of California, Berkeley, CA, USA*

² *Department of Environmental Sciences, Rutgers University, New Brunswick, NJ, USA*

Final accepted version for Geoscience Letters, November 2023

***Corresponding author**

John Chiang, Department of Geography, University of California, Berkeley CA 94720-4240 USA

jch_chiang@berkeley.edu

Manuscript is based on the Axford lecture given by the first author at the Asia-Oceania

Geoscience Society 20th annual meeting in Singapore, July 2023.

Abstract

The seasonality of Earth's climate is driven by two factors: the tilt of the Earth's rotation axis relative to the plane of its orbit (hereafter the *tilt effect*), and the variation in the Earth-Sun distance due to the Earth's elliptical orbit around the Sun (hereafter the *distance effect*). The seasonal insolation change between aphelion and perihelion is only $\sim 7\%$ of the annual mean and it is thus assumed that the distance effect is not relevant for the seasons. A recent modeling study by the authors and collaborators demonstrated however that the distance effect is not small for the Pacific cold tongue: it drives an annual cycle there that is dynamically distinct and $\sim \frac{1}{3}$ of the amplitude from the known annual cycle arising from the tilt effect. The simulations also suggest that the influence of distance effect is significant and pervasive across several other regional climates, in both the tropics and extratropics. Preliminary work suggests that the distance effect works its influence through the thermal contrast between the mostly-ocean hemisphere centered on the Pacific Ocean (the 'Marine hemisphere') and the hemisphere opposite to it centered over Africa (the 'Continental hemisphere'), analogous to how the tilt effect drives a contrast between the northern and southern hemispheres. We argue that the distance effect should be fully considered as an annual cycle forcing in its own right in studies of Earth's modern seasonal cycle. Separately considering the tilt and distance effects on the Earth's seasonal cycle provides new insights into the workings of our climate system, and of direct relevance to paleoclimate where there are outstanding questions for long-term climate changes that are related to eccentricity variations.

Keywords: Seasons, Orbital Eccentricity, Tropical ocean-atmosphere interactions

1. Introduction

Earth's climatic seasonal cycle is driven by two features of the Earth's orbit around the Sun: the tilt (obliquity) of the Earth's rotation axis relative to the plane of the orbit (hereafter referred to as the ***tilt effect***), and the variation in the Earth-Sun distance (***distance effect***). They introduce an seasonal variation in the insolation received by the Earth at any one point: the tilt through changing the angle of the sun's ray incident on the surface, and distance through changing the solar flux incident on the Earth, as the Earth progresses through its orbit. The Earth's orbit around the Sun (figure 1) is elliptical with the Sun at one focal point and with the closest approach at perihelion and furthest at aphelion; this provides the basis for the distance effect. The orbital eccentricity e (see figure 1 for a definition) is currently small at ~ 0.0167 , which means that the Earth-Sun distance at aphelion is $\sim 1.67\%$ longer than the mean Earth-Sun distance. Earth's rotation axis is tilted (currently at an angle of 23.5°) relative to the normal of the plane of the ecliptic (the path of Earth's orbit around the Sun). As the intensity of sunlight received by a given area depends on the angle of incidence that it makes with the Sun's incoming rays, this forms the basis of the tilt effect: at (northern hemisphere) winter solstice, the southern hemisphere surface is more face-on to the Sun's rays and thus receives more sunlight per unit area of surface, whereas it is the opposite for the northern hemisphere. During the summer solstice, the situation is reversed.

In practice, we are taught that our seasons are driven by the tilt effect, with the distance effect assumed to be negligible because seasonal insolation change between aphelion and perihelion is only $\sim 7\%$ given the small orbital eccentricity. A well-known college-level climatology textbook (Hildore et al. 2010) writes: "The amount of solar radiation intercepted by Earth at perihelion is about seven percent higher than at aphelion. This difference, however, is not the major process in producing the seasons." They go on to say that the "primary factor responsible for the hot and cold seasons as well as the wet and dry seasons is the revolution of the earth about the sun and the inclination of the earth's axis to its orbital plane." Other texts tell

a similar story. The entry on “Seasons” in the Encyclopedia of Climate and Weather (2nd Edition; Schneider et al. 2011) states that “Because the Sun’s output remains relatively fixed from day to day, the Earth receives about 3 percent more energy than the annual daily average from the Sun on the perihelion and about 3 percent less on the aphelion, not enough to explain the large seasonal temperature differences. That is why ellipticity in the orbit cannot be the fundamental cause of the seasons in the Northern Hemisphere. The actual cause of the observed seasons is the relative tilt of the Earth’s axis.”

The neglect of the distance effect in the seasons extends to the research literature on modern-day climate. There are relatively few studies that examine the seasonal cycle to begin with, with a greater emphasis placed on climate variations on shorter (e.g. Madden-Julian Oscillation) and longer timescales (e.g. El Niño-Southern Oscillation, Atlantic Multidecadal Oscillation). Within this existing literature, there are virtually no studies that critically examine the relative roles of tilt and distance in generating Earth’s seasons. A literature search by the authors managed to uncover only two studies that explicitly differentiate the role played by distance from that of tilt in the modern climate: Reid and Gage (1981) argued that the annual cycle of the tropical tropopause height is driven by orbital eccentricity, and Roach et al. (2023) argued that the observed hemispheric difference in the length of cooling and warming seasons results from orbital eccentricity. While there are likely to be others, the point we make is that such studies are rare.

The lack of consideration of the distance effect on Earth is in stark contrast to the study of seasonal climate of other planets, where both distance and tilt effects are given due consideration (e.g. Guendelman and Kaspi 2020). Studies of the Martian seasonal cycle provide a contrast. Several seasonal features on Mars are attributed to the distance effect (with aphelion occurring in late northern Spring) including a much stronger southern summer Hadley circulation, larger northern ice cap compared to the south, and an order of magnitude more dust devils in the southern hemisphere (Mischna 2018). We are led to an interesting situation where

we likely know more about the role of eccentricity in the seasonal climate of Mars than that of the Earth! While it is true that Mars' eccentricity is larger than that of Earth (at $e \sim 0.09$ around 5x larger), the difference does not seem so great as to justify full consideration of the distance effect in Mars' seasonality but virtually none for that of the modern Earth.

The role of eccentricity on Earth's seasons might be more prominent were the southern hemisphere to have continental area like in the northern hemisphere: since perihelion occurs near northern hemisphere winter solstice and aphelion during northern hemisphere summer solstice, seasonal contrasts in the southern hemisphere would have been more pronounced than in the northern hemisphere. However, because of the differences in continental land area between hemispheres, it is difficult to compare northern hemisphere seasons with those in the southern hemisphere.

The standard argument given in textbooks for neglecting the distance effect points to the relatively small 7% variation in seasonal insolation between aphelion and perihelion. However, whether this is small relative to the tilt effect depends on the latitude. Away from the deep tropics, the annual variation in insolation is indeed dominated by tilt (figure 2a). Near the equator however, the distance effect dominates the annual cycle of insolation, even though the larger variation is a semiannual cycle contributed by the tilt effect (figure 2b). Also, comparing insolation at a given latitude Earth assumes that it is the local insolation that determines the seasonal cycle. This might be true of surface temperature at many locations, but not necessarily so for other fields such as wind or precipitation, where the large-scale response of the climate system to the insolation change may be more important. If we take the globally averaged insolation to be relevant to earth's seasonality, then its seasonal cycle is entirely contributed by the distance effect (figure 2c).

The neglect of the distance effect in modern climate research is also in stark contrast to the robust literature on the climate effects of explosive volcanism, the latter being a climate forcing of a similar nature (global reduction of solar radiation) and timescale (months). The peak

monthly mean radiative forcing for the Mount Pinatubo eruption is about -3.2 W/m^2 (Schmidt et al. 2015), much smaller in magnitude compared to the decrease in the area-averaged insolation at aphelion (relative to the annual mean) of $\sim 8 \text{ W/m}^2$.

A notable exception in the climate literature on the role of the distance effect on Earth's seasons is a provocative claim by Thomson (1995) that Earth's seasons have a periodicity that follows the anomalistic year rather than the tropical year. The anomalistic year is based on the period between successive perihelia, currently 365.259636 days (United States Nautical Almanac Office, 2019). The tropical year is based on the period between successive equinoxes (365.242189 days) and is also the year that the Gregorian calendar is based on: the system of leap years brings the average calendar year to be very close to the tropical year, 365.2425 days (Thomson 1995). Thomson based his claim on a statistical analysis of the annual cycle phase in long-term weather station instrumental records: he showed that the longest station temperature record in existence - the Central England temperature record which started in 1619 - changes its phase with respect to the Gregorian calendar in accordance with what would be expected if the period of the annual cycle followed the anomalistic year. He also found that northern hemisphere records prior to 1940 changed phase on aggregate consistent with his hypothesis, though with large variation between stations. While Thomson (1995) received a lot of attention when it was first published, it also received immediate pushback (Karl et al. 1996) and the idea did not gain traction. Thomson's claim lacked a plausible mechanism: he invoked the 'FM capture' analogy whereby an FM receiver receiving two signals at similar frequency chose the one signal over the other but did not offer a reason as to why Earth's seasonality should behave in a similar way. The natural variability of phase changes in Earth's seasonality is also not well known but is needed to assess the significance of the phase changes found in Thomson's analysis. Regardless, we highlight Thomson (1995) as a rare example of a study that critically questioned the neglect of orbital eccentricity in the modern-day seasons.

2. Two annual cycles of the Pacific cold tongue

A recent study by the authors and collaborators (Chiang et al. 2022) on the seasonality of the Pacific cold tongue led the authors to reconsider the role of orbital eccentricity on Earth's seasons. We summarize this study as a motivation for our argument.

The Pacific cold tongue is a region of relatively cold sea surface temperatures (SST) in the eastern equatorial Pacific otherwise surrounded by warmer waters (figure 3). The region is best known as the epicenter of the El Niño-Southern Oscillation (ENSO) - during a El Niño event, the SST in the cold tongue region warms up, thus reducing the contrast with the surrounding tropical ocean and in particular the gradient in SST between the western and eastern equatorial Pacific. The reason for the existence of the cold tongue is well understood (Bjerknes 1969): easterly trades impinging on the equator push equatorial ocean surface waters to the west, shoaling the thermocline (the separation between the warm surface waters and the colder waters below) to the east. Equatorial upwelling over the eastern Pacific thus brings up relatively cold water, cooling the SST in the region, forming the cold tongue. The resulting east-west contrast in SST creates an atmospheric pressure gradient that enhances the initial easterly trades, thus resulting in a coupled ocean-atmosphere (Bjerknes) feedback that maintains the east-west asymmetry.

If the cold tongue were driven by a thermodynamic response to insolation it would possess a dominant semiannual cycle in SST since the Sun is directly overhead at the equator twice a year; but instead, the cold tongue seasonality is dominated by an annual cycle (Mitchell and Wallace 1992) (figure 3a). The prevailing understanding of the cold tongue annual cycle - developed in the 1990's (Mitchell and Wallace 1992, Xie 1994, Chang 1996) - points to the strength of the southeasterly trades crossing the equator as the key causal factor. The Intertropical Convergence Zone (ITCZ) is located north of the equator throughout the year (Philander et al. 1996), and so the southeasterly trades cross the equator from south to north. Stronger trades lead to colder SST through coastal upwelling propagated into the interior (Xie

1996, Nigam and Chao 1996) and increased turbulent mixing and surface fluxes (Chang 1996, Xie 1996). The strength of the southeasterly trades is driven by the seasonal variation in the interhemispheric temperature gradient - it is strongest in boreal Fall when the northern hemisphere SST peaks and southern hemisphere SST is at a minimum, and vice versa (figure 3b, c) - and hence the cold tongue SST is coldest in September-October and warmest in March-April. Thus, it is ultimately the tilt effect that creates the annual cycle of the Pacific cold tongue SST.

An Earth System model study of Pacific cold tongue seasonal cycle response to precession by Erb et al. (2015) produced remarkable results that challenged this prevailing understanding. They set the eccentricity in their simulations to a relatively large value ($e = 0.0493$, the maximum that Earth's eccentricity attained over the last 600,000 years) and vary the longitude of perihelion (LOP; see figure 1 for a definition); they also set the obliquity to preindustrial (23.439°). When perihelion was specified to occur during the winter solstice (90° - close to where it is today), the model simulated a cold tongue annual cycle that is like today's - cold during September and warm in April (figure 4a). However, as the longitude of perihelion increases, the phasing of the cold tongue changes dramatically such that the timing of the warm and cold periods migrates across the calendar year (figure 4b-d). The amplitude of the seasonal cycle also noticeably changes, with a more muted amplitude for perihelion at autumnal equinox (figure 4d). This contrasts with prevailing theory that would have predicted that the cold tongue seasonal cycle remains the same in all simulations, since obliquity was fixed. Curiously, a further simulation in Erb et al. (2015) setting eccentricity to zero yielded a cold tongue seasonal cycle with phasing like present-day (figure 4e). Chiang et al. (2022) reproduced this result for several other model simulations, indicating that the change in the cold tongue is robust.

Chiang et al. (2022) solved this problem by undertaking a set of simulations with an Earth System model (see section 6 for details) spanning the space of eccentricity (from 0 to

0.04) and longitude of perihelion (LOP in steps of 30°), to map out the behavior of the cold tongue seasonal cycle under precession. The obliquity was fixed to the preindustrial value of 23.439° . They fitted the simulated monthly mean cold tongue SST seasonal cycle with the longitude of perihelion with a sum of three cosines, one representing the annual cycle from the tilt effect, another the annual cycle from the distance effect, and third being the semiannual cycle arising from the tilt effect:

$$CT_{fit} = A_T \cos \left(\left(\frac{2\pi}{12} \right) (m - p_T) \right) + A_D \cos \left(\left(\frac{2\pi}{12} \right) (m - p_D) - \left(\frac{LOP\pi}{180} \right) \right) + A_S \cos \left(\left(\frac{2\pi}{6} \right) (m - p_S) \right) \quad [1]$$

where A_T and p_T are the amplitude and phase of the annual cycle for the **Tilt** effect; likewise, A_D and p_D for the **Distance** effect, and A_S and p_S for the **Semiannual** cycle from the tilt effect. m is the numerical months of the year from 0 to 12 (with 0.5 corresponding to mid-January), and LOP is the longitude of perihelion, in degrees (see section 6 for details of this calculation). They found that this model fits the data well, and the resulting decomposition showed that cold tongue seasonal cycle had significant contributions from both the tilt and distance effect annual cycles (figure 5); by comparison, the tilt effect semiannual cycle was small. The tilt effect annual cycle had an amplitude of around 1.1K and with the warm period around April-May and the cold period in September-October, consistent with the prevailing theory of the cold tongue seasonal cycle. The distance effect annual cycle possessed an amplitude that increasing linearly with eccentricity at a rate of around ~ 0.23 K per 0.01 eccentricity units, and a phasing that changed linearly with the longitude of perihelion. ***This meant that the cold tongue possesses not one but two annual cycles:*** one driven by tilt and in accordance with the prevailing theory, and the other being a heretofore undiscovered annual cycle driven by the distance effect. The amplitude of the distance effect annual cycle is comparable with that of tilt for the largest eccentricities experienced by Earth ($e \sim 0.05$); even at today's relatively small eccentricity ($e \sim 0.0167$) the distance effect annual cycle amplitude is $\sim 1\%$ of the tilt effect - in other words, it is

not negligible! As we will discuss in section 3, the distance-effect annual cycle of the cold tongue is not simply a thermodynamic response to insolation, but a *dynamical* one.

Since the distance-effect annual cycle has the period of the Anomalistic year, which is about ~25 minutes longer than the period of the tilt effect annual cycle (which follows the Tropical year), over time the phase of the distance-effect annual cycle shifts relative to the tilt effect annual cycle. Thus, the Pacific cold tongue behavior seen by Erb et al. (2015) is readily explained as the result of the superposition of two annual cycles of comparable amplitudes but with slightly different periods - as perihelion shifts from vernal equinox to autumnal equinox, the two annual cycles go from being in phase and reinforcing, to being out of phase and canceling (compare figure 5d with 5e). As such, the cold tongue annual cycle amplitude is large for perihelion at the vernal equinox and small during the autumnal equinox (figure 4).

It could be argued that the Pacific cold tongue is a special case for being influenced by eccentricity, as it is located at the equator where the seasonal insolation from the distance effect is relatively strong (figure 2b). However, an examination of the simulations in Chiang et al. (2022) but for other climate fields shows that other regional climates possess a strong imprint of the distance effect in their annual cycle. We show this by calculating - for each gridpoint in the model space - the ratio of the distance effect amplitude to the tilt effect amplitude, derived from a fit to equation 1. This calculation was done using the CESM LOP simulations of Chiang et al. (2022) with $e = 0.02$, an eccentricity only slightly higher than today's levels (see section 6 for details).

Figure 6a shows this calculation for surface temperature, and we highlight areas with ratios 20% and larger (in other words, the distance effect amplitude is at least $\frac{1}{5}$ that of the tilt effect). The ratio is below 20% for all the extratropics, indicating the dominance of the tilt effect. However, the ratio is above 20% for most of the tropical continents, which suggests a direct insolation influence of the distance effect on the surface temperature annual cycle. This ratio is also above 20% over much of the tropical oceans and there is a structure to it suggesting a

dynamical influence: apart from the Pacific cold tongue region which we are already familiar with, the ratio is large over the Indian ocean to the north and south of the equator, and over the equatorial Atlantic north of the equator. The same calculation but for 500mb geopotential height shows that the influence of distance is pervasive over the tropical troposphere (figure 6b), consistent with the observation by Reid and Gage (1981) that the seasonal cycle of tropical tropopause height is driven by eccentricity. The distance effect for surface temperature is relatively large over regions of deep convection: Central Africa, the Maritime Continent, and tropical South America (figure 6a), which would explain the strong distance effect contribution for 500mb geopotential height given that tropical tropospheric temperature variations are controlled by the surface temperature of deep convective regions (Sobel and Bretherton 2000).

The distance effect contributes significantly to the annual cycle in the extratropics for some fields. For rainfall (figure 6c), the distance contribution is significant over tropical Africa and the Maritime Continent. However, there are extratropical locations where the distance effect amplitude is significant, including North Africa, Hawaii, and the region around New Zealand. Examination of the same ratio but for zonal wind stress (figure 6d) shows changes over Central Africa and neighboring the Maritime continent. However, the most noticeable contribution is over the South Pacific midlatitude westerlies, where the distance effect amplitude is comparably as large as that for the tilt effect. Thus, the distance effect has a pervasive influence on seasonality, not just in the tropics but also the extratropics.

3. The distance-effect annual cycle of the Earth

The lesson we learn from Chiang et al. (2022) is that the distance effect should be treated as an annual cycle forcing in its own right. What we mean by this statement is that one should account for both annual cycles in seasonal cycle studies, separate their respective roles, and give the annual cycle from distance the same due consideration as for tilt. For example, the characteristic seasonal response from the tilt effect is generally conceptualized as the migration

of the ITCZ in response to the contrasting temperature evolution between the northern and southern hemispheres, with the associated Hadley cells and westerlies migrating in unison.

What is the equivalent picture for the distance-effect annual cycle?

As discussed in Chiang et al. (2022), we propose that the distance effect also appears to act through contrasting hemispheres, but in this case between the hemisphere centered over the Pacific (the '*Marine hemisphere*' because of the prevalence of ocean) with the hemisphere opposite it (the '*Continental hemisphere*' because of the prevalence of land) (figure 7). This response is expressed as an east-west hemispheric pattern in surface pressure as well as the upper tropospheric velocity potential (figure 8), and it leads to a seasonal zonal shift of the Walker uplift region. We call this the 'zonal monsoon' as it causes a seasonal zonal wind reversal over the Maritime continent, with stronger easterlies during equatorial summer and weak westerlies during equatorial winter.

The hemispheric response comes about because of the differential thermal response between the Marine and Continental hemispheres (Chiang et al. 2022). An energy contrast is generated between the two hemispheres such that in the months leading up to and following perihelion, the surface of the Marine hemisphere absorbs more energy than that of the Continental hemisphere. Because the tropical atmosphere cannot maintain large temperature gradients (Sobel et al. 2001), energy is fluxed by the atmosphere from the Continental to the Marine hemisphere through the zonal overturning circulation, resulting in a shift in the Walker uplift region westward towards the Continental Hemisphere. In the months leading up to and following aphelion, the opposite occurs. Thus, the characteristic tropical circulation response to the distance effect is a seasonal east-west shift of the Walker circulation.

This Walker shift also leads to the generation of the distance-effect cold tongue annual cycle found in Chiang et al. (2022). The seasonal shift in the Walker uplift region causes an annual cycle in the strengthening and weakening of the easterly trades in the western equatorial Pacific, that in turn forces a coupled ocean-atmosphere response like what is seen for ENSO,

except that it is periodically forced (Chiang et al. 2022). Hence, the same dynamics that generates the El Niño-Southern Oscillation also produces the distance-effect annual cycle of the cold tongue.

We note an interesting symmetry in the seasonal tropical circulation response between the distance and tilt effects, in that both are the consequence of interhemispheric contrasts. For the tilt effect, the thermal contrast between the northern and southern hemispheres drives a global monsoon, and the latitudinal position of the ITCZ shifts to accommodate the meridional atmospheric energy transport between hemispheres (Chiang and Friedman 2012) (figure 7b). For the distance effect, the thermal contrast between the Continental and Marine hemispheres drives a zonal monsoon, and the longitudinal position of the Walker uplift shifts to accommodate the zonal atmospheric energy transport between hemispheres (Chiang et al. 2022).

Finally, we showed in figure 6 that the seasonal variation in some regional extratropical climates have a disproportionate contribution from the distance effect, despite the dominance of the tilt effect in the seasonal insolation received in those regions. We speculate that the seasonal Walker shift is likely to give rise to stationary Rossby waves in both hemispheres, akin to the global teleconnections from an El Niño event: this provides a mechanism by which the distance effect felt in the deep tropics can contribute to the annual cycle of extratropical climates. How the distance effect annual cycle is phased relative to the tilt effect (i.e., the longitude of perihelion) will strongly influence this teleconnection, since stationary waves are more readily generated in the winter hemisphere (Trenberth et al. 1998). In general, the net seasonally that combines the tilt and distance effects will also crucially depend on the longitude of perihelion.

4. Implications for Paleoclimate

Chiang et al. (2022) illustrates how separately considering the distance and tilt effects on the annual cycle in regional climates leads to new insights into Earth's seasonal cycle and

underlying mechanisms. The cold tongue annual cycle driven by the distance effect is, however, a model prediction and thus requires testing. This is where seasonally resolved proxies such as oxygen isotopic records from corals or molluscs become essential. For regions where there is a substantial distance effect annual cycle (such as the cold tongue), the net annual cycle will vary both in amplitude and phase over a precessional cycle as the tilt and distance-effect annual cycles combine and interfere.

For the cold tongue, the mid-Holocene period is a good target as the perihelion was close to the autumnal equinox (LOP $\sim 0^\circ$) around 6000 ybp, and the two annual cycles were out of phase and canceling (cf figure 5a); indeed, a markedly reduced cold tongue annual cycle has been observed in past modeling studies of the mid-Holocene (Luan et al. 2012, Karamperidou et al. 2015). In terms of proxy observations, a study by Koutavas and Joanides (2012) sampling oxygen isotopic ratios (a proxy of sea surface temperature) from individual foraminifera data in the heart of the cold tongue showed an intriguing dip in its variance during the mid-Holocene, in apparent support of the model prediction. However, it is not straightforward to separate the ENSO and seasonal cycle contributions to this signal: Koutavas and Joanides (2012) interpret the data to reflect a reduction to ENSO amplitude, but Thirumalai et al. (2013) instead argues on statistical grounds that the data more likely reflects a reduction to the seasonal cycle amplitude. Proxy annual cycle observations from seasonally resolved oxygen isotopic reconstructions from corals and molluscs have however been equivocal: a synthesis study by Emile-Geay et al. (2015) report that those data exhibit little coherence through the Holocene. For the eastern Pacific, proxies generally show a slightly reduced annual cycle amplitude throughout the past 10kyr compared to today, whereas the central Pacific shows either similar or increased annual cycle amplitude to today in the mid-Holocene but with large variation.

The more interesting paleoclimate test for the cold tongue would be on the calendar phase of its annual cycle: during which months is the cold tongue at its warmest or coldest? However, this requires the difficult task of affixing the calendar to the paleorecord - in other

words, the position of the equinoxes and solstices. The authors are not aware of any proxy that does this, and we hope that the results of Chiang et al. (2022) will motivate the development of such paleoproxy methods. One potential way forward for cold tongue proxies is through resolving the semiannual cycle, as those are tied to the equinoxes. In general, our call to focus on seasonality is in line with increased emphasis on reconstructing seasonality in paleoclimate records (Carre and Cheddadi 2017). We note that tropical Pacific paleoclimate studies are typically geared towards addressing ENSO, but the modeling results of Chiang et al. (2022) suggest that more emphasis should be placed on the seasonal cycle: its variations are potentially larger, and more importantly predictable.

Understanding distance effect on our seasonal climate and especially on regional scales is clearly needed to advance our knowledge of paleoclimate on orbital timescales, and especially given the fact that the annual mean insolation is only very weakly dependent on eccentricity. Our current eccentricity ($e = 0.0167$) is relatively low - over the last million years, the average eccentricity has been 0.0281, with a maximum of 0.0578 (Laskar et al. 2011) - so the potential is there for eccentricity to manifest itself more strongly in the seasonal cycle. There are several outstanding paleoclimate questions that involve eccentricity, for example the classic problem of glacial-interglacial cycles where a basic tenet of the Milankovitch hypothesis is based on seasonality: that there is less ice growth during warmer summers. There is also the intriguing case of the Last Interglacial climate, which has been shown to be distinctly warmer by $\sim 1.5^\circ\text{C}$ (Turney and Jones 2010, McKay et al. 2011) and with 6 - 9m higher sea level compared to modern (Hearty et al. 2007, Kopp et al. 2009) even though the Last Interglacial has similar CO₂ levels as preindustrial. Interestingly, climate models do not simulate a warmer Last Interglacial despite the larger eccentricity imposed (Otto-Bliesner et al. 2013, Otto-Bliesner et al. 2021). We contrast these outstanding paleoclimate questions with the fact that the relative roles of distance and tilt in the seasonality of our modern climate is essentially unexplored. Bringing the tools of modern climate studies to bear on understanding the relative roles of tilt and

eccentricity on Earth's seasons will benefit paleoclimate studies, through providing a more comprehensive view of the origins of seasonality and how it changes and making the connection between climate dynamics and paleoclimate.

We highlight a potential problem on how the distance effect on Earth's seasonality is currently conceptualized in paleoclimate. The climate effect of eccentricity is commonly interpreted as a modulation of the tilt effect annual cycle: for example, the enhancement of the North African rainfall in the early-mid Holocene is explained as a response of the monsoon to increased summer insolation due to perihelion occurring near the northern hemisphere summer solstice (Kutzbach and Liu 1997). The underlying assumption here is that distance effect on North African rainfall seasonality works through the same dynamics as for the tilt effect. This assumption is however incorrect if applied to the Pacific cold tongue changes in Chiang et al. (2022), as the distance-effect annual cycle of the cold tongue arises from dynamics distinctly different from that of the tilt-effect annual cycle. This example reinforces our suggestion that the distance and tilt effects be viewed as two distinct annual cycles that superpose to produce the net seasonal cycle, rather than the distance effect being a modulation of the tilt effect.

5. How do we put eccentricity back into seasons?

Why is there a lack of attention in the modern climate literature to the distance effect on Earth's seasonal climate? There is a cultural/historical aspect to this: the notion of four seasons is a perspective coming from the northern hemisphere midlatitudes and defined by the timing of solstice and equinoxes: northern hemisphere summer is from summer solstice to autumnal equinox, northern hemisphere autumn from autumnal equinox to winter solstice, and so forth. Thus, the prevailing view of the seasons is based on the tilt effect, with the timing accounting for thermal lag from the oceans that delayed the peak warming relative to peak insolation. In the Tropics the temperature variations are much smaller, and the seasons are instead defined by wet and dry periods arising from monsoons. The monsoons are however also a product of the

tilt effect: the interhemispheric gradient in temperature generated from tilt drives cross-equatorial monsoonal flows that makes the warmer hemisphere wetter.

High school and college science education may have inadvertently played a role. There is a popular misconception that the seasons arise from the changing Earth-Sun distance, as highlighted in the well-known educational documentary 'A Private Universe' (Schneps and Sadler, 1989). The documentary shows that private (and incorrect) ideas on basic scientific concepts like the seasons are hard to dispel even when taught in the classroom; and thus, countering such preconceived ideas has been a focus of science education. We speculate that this effort may have inadvertently led to eccentricity not being given its proper due in studies of seasonality in the modern climate literature.

If this is indeed the case, it suggests that we should seek ways to reintroduce eccentricity into our teaching of Earth's seasonal cycle, but in a way that does not discount the primacy of the tilt effect. One way to do so is to deepen our teaching of the seasons to highlight areas where the distance-effect does play a role in the modern-day seasons: an example could be the difference in the length of warming and cooling seasons between the northern and southern hemispheres, as found by Roach et al. (2023). Another way is to remind students that Earth's seasons ultimately originate from the seasonal variation of insolation received at the top of the atmosphere, and which has contributions from both Earth's axial tilt and orbital eccentricity.

Finally, we suggest a greater effort towards research on the dynamical origins of seasonality. Seasonality is relatively understudied compared to interannual/decadal variability and trends, even though the seasonal variations are much larger (Jennings and Magrath 2009). The seasons are how most people experience climate, and they profoundly affect how they live (Orlove 2003). A seasonal perspective is more easily relatable to people's perceptions of climate change (Sparks and Menzel 2002) and presents a more effective way to communicate climate: for example, Lukovic et al. (2021) found a significant downward trend in November

averaged rainfall in California station data since the 1960's, but this result is much easier communicated as a progressive delay in the onset of the California winter rainy season. As exemplified by the findings in Chiang et al. (2022), there are still mysteries to be solved on the workings of the Earth's seasonal cycle.

6. Appendix

The data used for the calculations in figure 5 and figure 6 are the CESM LOP simulations of Chiang et al. (2022); a brief description follows, and the reader is referred to Chiang et al. (2022) for additional details. Simulations are done with Community Earth System Model (CESM) 1.2 (Hurrell et al. 2013) at $1.9^\circ \times 2.5^\circ$ finite-volume grid and ocean and sea ice on a nominal 1° rotated pole grid (gx1v6). Each simulation is for 25 model years, and the last 20 years are averaged to form a seasonal climatology. Simulations span the space of eccentricity and LOP: eccentricity is simulated for $e=0, 0.01, 0.02$ and 0.04 ; and LOP is varied at intervals of 30° from 0° to 330° . All other boundary conditions are set to pre-industrial levels, including obliquity which is fixed to 23.439° .

For figure 5, an index of the monthly mean climatological seasonal cycle of the cold tongue is created for each simulation case by averaging monthly climatological surface temperature over $6^\circ \text{S} - 6^\circ \text{N}$, $140^\circ\text{W} - 90^\circ\text{W}$; its annual mean is subsequently subtracted out. For each eccentricity case ($0, 0.01, 0.02, 0.03, 0.04$), we fit the simulated seasonal cycle to equation 1 (equation reproduced below for convenience):

$$CT_{fit} = A_T \cos\left(\left(\frac{2\pi}{12}\right)(m - p_T)\right) + A_D \cos\left(\left(\frac{2\pi}{12}\right)(m - p_D) - \left(\frac{LOP\pi}{180}\right)\right) + A_S \cos\left(\left(\frac{2\pi}{6}\right)(m - p_S)\right)$$

It is the sum of 3 cosines, the first representing the tilt effect annual cycle (T), the second the distance effect annual cycle (D), and the third the tilt effect semiannual cycle (S). The cosine representing the distance effect has phase change that is linear with the longitude of perihelion (LOP), since the months are timed to the year defined by the tilt (Tropical year). Time in months

is represented by 'm' being 0.5 for January, 1.5 for February etc. LOP is the longitude of perihelion in degrees.

There are 6 parameters to fit: three amplitudes A_T , A_D , and A_S , and three phases p_T , p_D , and p_S for the tilt effect annual cycle, distance effect annual cycle, and tilt effect semiannual cycle respectively. The surface fit using equation (1) is done in MATLAB R2021a using the function 'fit' and specifying equation (1) as the model using the function 'fittype', setting m and LOP as the independent variables; otherwise, default settings are used. Both functions are found in the curve fitting toolbox. The method uses a nonlinear least squares minimization algorithm (trust-region reflective method) to determine the fit. For the $e = 0$ case, A_D is assumed to be zero. Figure 5b illustrates the fit to the simulation data for the $e = 0.04$ case shown in figure 5a, and figure 5d-f shows the tilt effect annual cycle, distance effect annual cycle, and tilt effect semiannual cycle contributions to the fit, respectively.

For the ratio of amplitudes $A_D:A_T$ in figure 6, a similar fit is done using equation (1) but for each gridpoint of the given climate field climatological annual cycle varying the longitude of perihelion. Only the $e = 0.02$ case is used.

7. List of abbreviations

CESM: Community Earth System Model

ENSO: El Niño-Southern Oscillation

ITCZ: Intertropical Convergence Zone

LOP: Longitude of Perihelion

SST: Sea surface temperature

8. Declarations

Availability of data and materials

Model output used in this study is the same as in Chiang et al. (2022) and is archived in Chiang, J. C. H., Vimont, D. J., Nicknish, P. A., Roberts, W. H. G. & Tabor, C. R. Data and Code associated with: two annual cycles of the Pacific cold tongue under orbital precession. *Dryad* <https://doi.org/10.6078/D1VB0G> (2022).

Competing interests

The authors declare that they have no competing interests.

Funding

JCHC acknowledges support from NSF AGS 2303385. AOGS covered the publication fee/article processing charge for this article.

Authors' contributions

JCHC and AJB conceived the topic and framing of the article, and JCHC led the writing of the manuscript with contribution by AJB. JCHC undertook all calculations and figures in this manuscript.

Acknowledgements

We thank the Asia-Oceania Geosciences Society (AOGS) for inviting us to contribute this article as part of the Axford lecture given by the first author (JCHC) at the AOGS 2023 20th annual meeting in Singapore.

9. References

Bjerknes, J., 1969. Atmospheric teleconnections from the equatorial Pacific. *Monthly weather review*, 97(3), pp.163-172.

Chang, P., 1996. The role of the dynamic ocean-atmosphere interactions in tropical seasonal cycle. *Journal of climate*, 9(12), pp.2973-2985.

Chiang, J.C., Atwood, A.R., Vimont, D.J., Nicknish, P.A., Roberts, W.H., Tabor, C.R., and Broccoli, A.J., 2022. Two annual cycles of the Pacific cold tongue under orbital precession. *Nature*, 611(7935), pp.295-300.

Chiang, J.C.H. and Friedman, A.R., 2012. Extratropical cooling, interhemispheric thermal gradients, and tropical climate change. *Annual Review of Earth and Planetary Sciences*, 40, pp.383-412.

Cronin, T.M., 2009. *Paleoclimates: understanding climate change past and present*. Columbia University Press.

Dee, D.P., Uppala, S.M., Simmons, A.J., Berrisford, P., Poli, P., Kobayashi, S., Andrae, U., Balmaseda, M.A., Balsamo, G., Bauer, D.P. and Bechtold, P., 2011. The ERA-Interim reanalysis: Configuration and performance of the data assimilation system. *Quarterly Journal of the royal meteorological society*, 137(656), pp.553-597.

Erb, M.P., Broccoli, A.J., Graham, N.T., Clement, A.C., Wittenberg, A.T. and Vecchi, G.A., 2015. Response of the equatorial Pacific seasonal cycle to orbital forcing. *Journal of climate*, 28(23), pp.9258-9276.

Hildore, J.J., Oliver, J.E., Snow, M., and Snow, R. Climatology: an atmospheric science. 3rd edition. Pearson Prentice-Hall, Upper Saddle River, New Jersey 07458, 416pp.

Huffman, G.J., Bolvin, D.T., Nelkin, E.J., Wolff, D.B., Adler, R.F., Gu, G., Hong, Y., Bowman, K.P. and Stocker, E.F., 2007. The TRMM multisatellite precipitation analysis (TMPA): Quasi-global, multiyear, combined-sensor precipitation estimates at fine scales. *Journal of hydrometeorology*, 8(1), pp.38-55.

Hurrell, J.W., Holland, M.M., Gent, P.R., Ghan, S., Kay, J.E., Kushner, P.J., Lamarque, J.F., Large, W.G., Lawrence, D., Lindsay, K., and Lipscomb, W.H., 2013. The community earth system model: a framework for collaborative research. *Bulletin of the American Meteorological Society*, 94(9), pp.1339-1360.

Huybers, P., and Eisenman, I., 2006. Integrated summer insolation calculations. NOAA/NCDC Paleoclimatology Program Data Contribution #2006-079.

Karamperidou, C., Di Nezio, P.N., Timmermann, A., Jin, F.F. and Cobb, K.M., 2015. The response of ENSO flavors to mid-Holocene climate: implications for proxy interpretation. *Paleoceanography*, 30(5), pp.527-547

Karl, T.R., Jones, P.D., Knight, R.W., White, O.R., Mende, W., Beer, J., and Thomson, D.J., 1996. Testing for bias in the climate record. *Science*, 271(5257), pp.1879-1879.

Koutavas, A. and Joanides, S., 2012. El Niño–Southern oscillation extrema in the holocene and last glacial maximum. *Paleoceanography*, 27(4).

Kutzbach, J.E. and Liu, Z., 1997. Response of the African monsoon to orbital forcing and ocean feedbacks in the middle Holocene. *Science*, 278(5337), pp.440-443.

Laskar, J., Fienga, A., Gastineau, M. and Manche, H., 2011. La2010: a new orbital solution for the long-term motion of the Earth. *Astronomy & Astrophysics*, 532, p.A89.

Luan, Y., Braconnot, P., Yu, Y., Zheng, W. and Marti, O., 2012. Early and mid-Holocene climate in the tropical Pacific: seasonal cycle and interannual variability induced by insolation changes. *Climate of the Past*, 8(3), pp.1093-1108

Luković, J., Chiang, J.C.H., Blagojević, D. and Sekulić, A., 2021. A later onset of the rainy season in California. *Geophysical Research Letters*, 48(4), p.e2020GL090350.

Mischna, M.A., 2018. Orbital (climatic) forcing and its imprint on the global landscape. In *Dynamic Mars* (pp. 3-48). Elsevier.

Mitchell, T.P. and Wallace, J.M., 1992. The annual cycle in equatorial convection and sea surface temperature. *Journal of Climate*, 5(10), pp.1140-1156.

Nigam, S. & Chao, Y. Evolution dynamics of tropical ocean–atmosphere annual cycle variability. *J. Clim.* 9, 3187–3205 (1996).

Philander, S. G. H. et al. Why the ITCZ is mostly north of the equator. *J. Clim.* 9, 2958–2972 (1996).

Roach, L.A., Eisenman, I., Wagner, T.J. and Donohoe, A., 2023. Asymmetry in the Seasonal Cycle of Zonal-Mean Surface Air Temperature. *Geophysical Research Letters*, 50(10), p.e2023GL103403.

Reid, G.C. and Gage, K.S., 1981. On the annual variation in height of the tropical tropopause. *Journal of Atmospheric Sciences*, 38(9), pp.1928-1938.

Schmidt, A., Mills, M.J., Ghan, S., Gregory, J.M., Allan, R.P., Andrews, T., Bardeen, C.G., Conley, A., Forster, P.M., Gettelman, A. and Portmann, R.W., 2018. Volcanic radiative forcing from 1979 to 2015. *Journal of Geophysical Research: Atmospheres*, 123(22), pp.12491-12508.

Schneider, S.H., 2011. *Encyclopedia of climate and weather*(Vol. 1). Oxford University Press.

Schneps, M. and Sadler, P.M., 1989. A private universe [Video]. Santa Monica, CA: Pyramid Film and Video.

Sobel, A.H., and Bretherton, C.S., 2000. Modeling tropical precipitation in a single column. *Journal of climate*, 13(24), pp.4378-4392.

Sobel, A.H., Nilsson, J. and Polvani, L.M., 2001. The weak temperature gradient approximation and balanced tropical moisture waves. *Journal of the atmospheric sciences*, 58(23), pp.3650-3665.

Thirumalai, K., Partin, J.W., Jackson, C.S. and Quinn, T.M., 2013. Statistical constraints on El Niño Southern Oscillation reconstructions using individual foraminifera: A sensitivity analysis. *Paleoceanography*, 28(3), pp.401-412.

Thomson, D.J., 1995. The seasons, global temperature, and precession. *Science*, 268(5207), pp.59-68.

Trenberth, K.E., Branstator, G.W., Karoly, D., Kumar, A., Lau, N.C. and Ropelewski, C., 1998. Progress during TOGA in understanding and modeling global teleconnections associated with tropical sea surface temperatures. *Journal of Geophysical Research: Oceans*, 103(C7), pp.14291-14324

United States Nautical Almanac Office, United States Naval Observatory, Her Majesty's Nautical Almanac Office and the United Kingdom Hydrographic Office. *The Astronomical Almanac for the Year 2019* (United States Government Printing Office, 2019).

Xie, S.P., 1994. On the genesis of the equatorial annual cycle. *Journal of Climate*, 7(12), pp.2008-2013.

Xie, S. P. Westward propagation of latitudinal asymmetry in a coupled ocean–atmosphere model. *J. Atmos. Sci.* 53, 3236–3250 (1996).

10. Figures

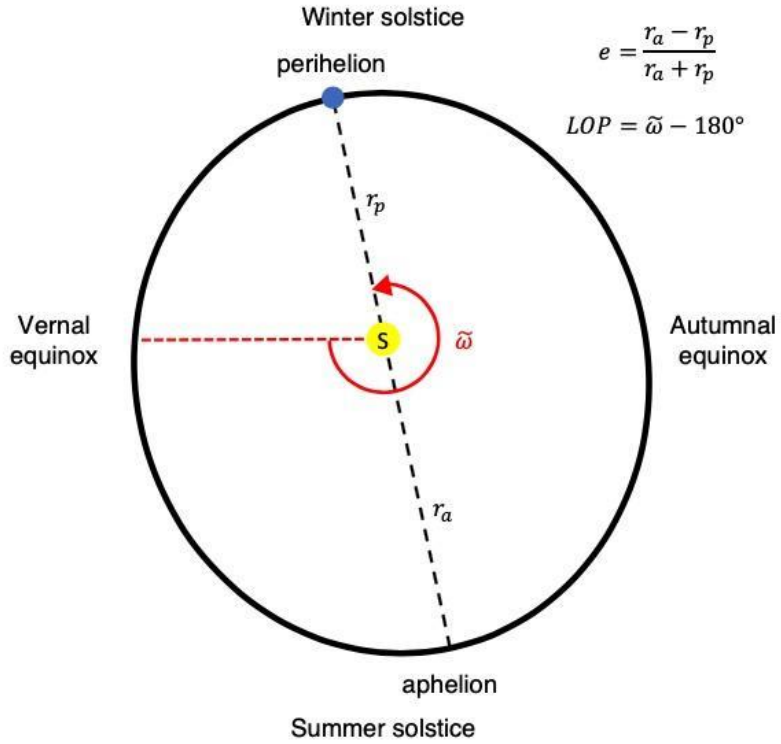


Figure 1: A schematic of the Earth's orbit around the Sun. The Earth's orbit is elliptical with the Sun (S) at one focal point and with the closest approach at perihelion (at a distance r_p) and furthest at aphelion (r_a). The direction of the orbit is counterclockwise. The eccentricity e , defined in the figure, measures how elliptical the orbit is; currently, $e = 0.01671$. The equinox and solstice points are named following Northern hemisphere seasons. The longitude of perihelion (LOP) relative to the moving vernal equinox is defined as the angular distance from vernal equinox to perihelion following Earth's orbit ($\tilde{\omega}$, in degrees), subtracted by 180° . Perihelion, as drawn in the schematic, is positioned for modern day, with an LOP of about 103° and date of around 3 January. Figure and caption adapted from Chiang et al. (2022), figure 1.

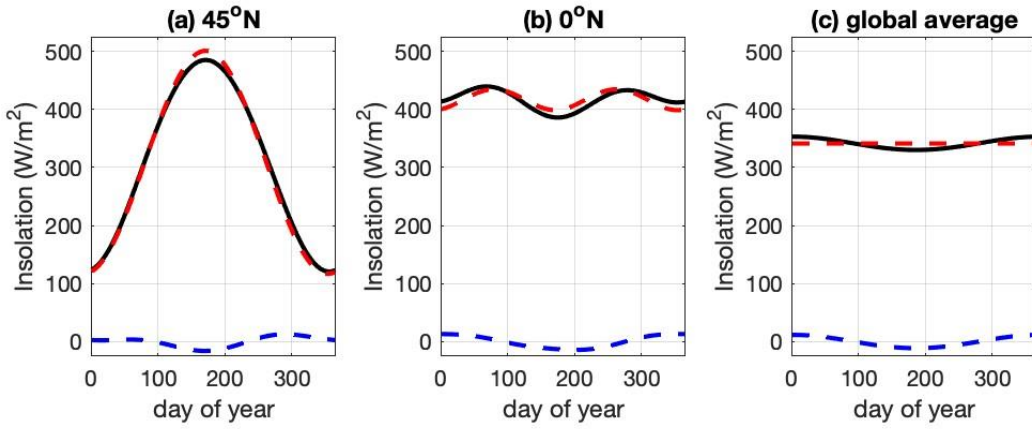


Figure 2: Comparison between the tilt and distance effect on incoming solar radiation (insolation). (a) Insolation at 45°N ; (b) Insolation at the equator, and (c) globally averaged insolation. The black solid line is the total insolation received, and the red dashed line is the insolation with $e = 0$ (tilt contribution); the difference is the distance contribution, shown in the blue dashed line. Insolation calculated using the code from Huybers and Eisenmann (2006), using preindustrial orbital parameters stated in Erb et al. (2015): $e = 0.0167$, obliquity = 23.439° , and longitude of perihelion = 102.932° .

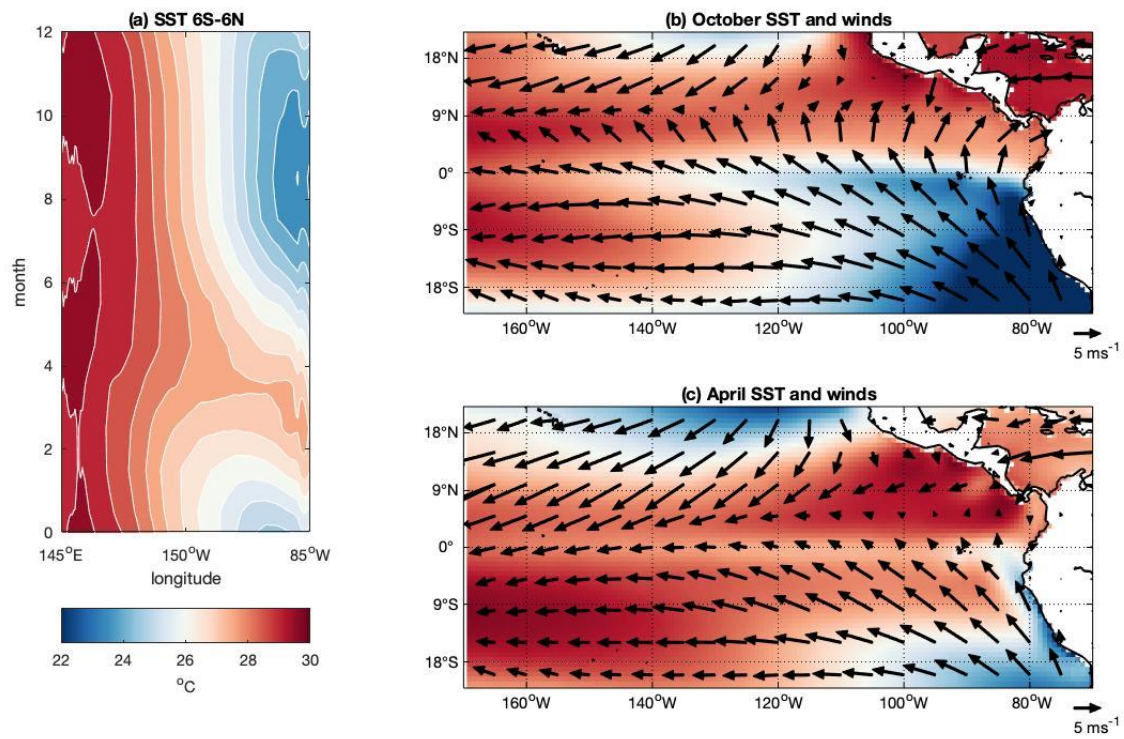


Figure 3. The Pacific cold tongue annual cycle. **a)** SST averaged over 6°S – 6°N , showing the cold tongue annual cycle with the cold peak in boreal fall and warm peak in boreal spring. Note that the time axis is such that 0 is the start of the year and 12 is the end; mid-January is thus 0.5. **(b-c)** SST and 10m winds for **(b)** October (cold peak), and **(c)** April (warm peak). Data is from ERA-Interim (Dee et al. 2011), averaged over 1979–2018. Figure taken from Chiang et al. (2022), Extended Data Figure 1.

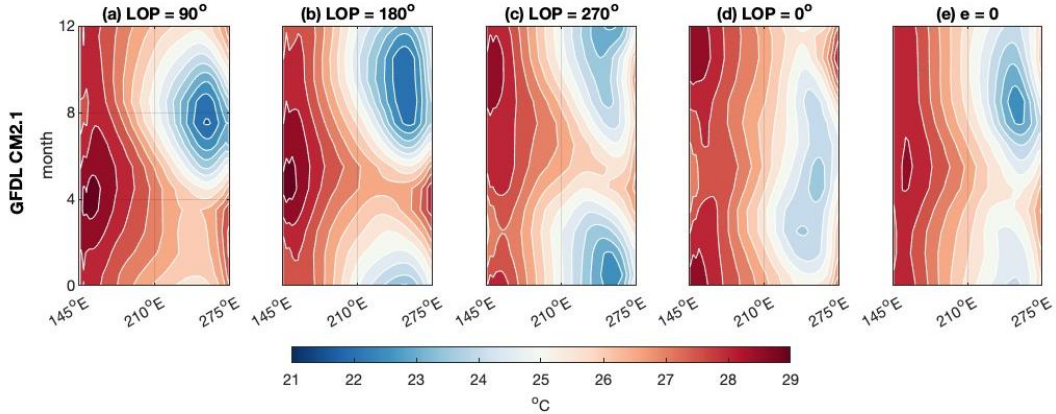


Figure 4. Change in cold tongue seasonality with the longitude of perihelion in Erb et al. (2015). Climatological monthly mean SST averaged over 6° S – 6° N across the Pacific basin (145°E – 275°E) for (a) perihelion at northern hemisphere winter solstice (LOP = 90°); (b) perihelion at vernal equinox (LOP = 180°); (c) perihelion at northern hemisphere summer solstice (LOP = 270°); and (d) perihelion at autumnal equinox (LOP = 0°). (e) shows the simulation with eccentricity set to zero ($e = 0$). Note that the month axis here is such that 0 is the start of the year and 12 is the end; mid-January is thus 0.5.

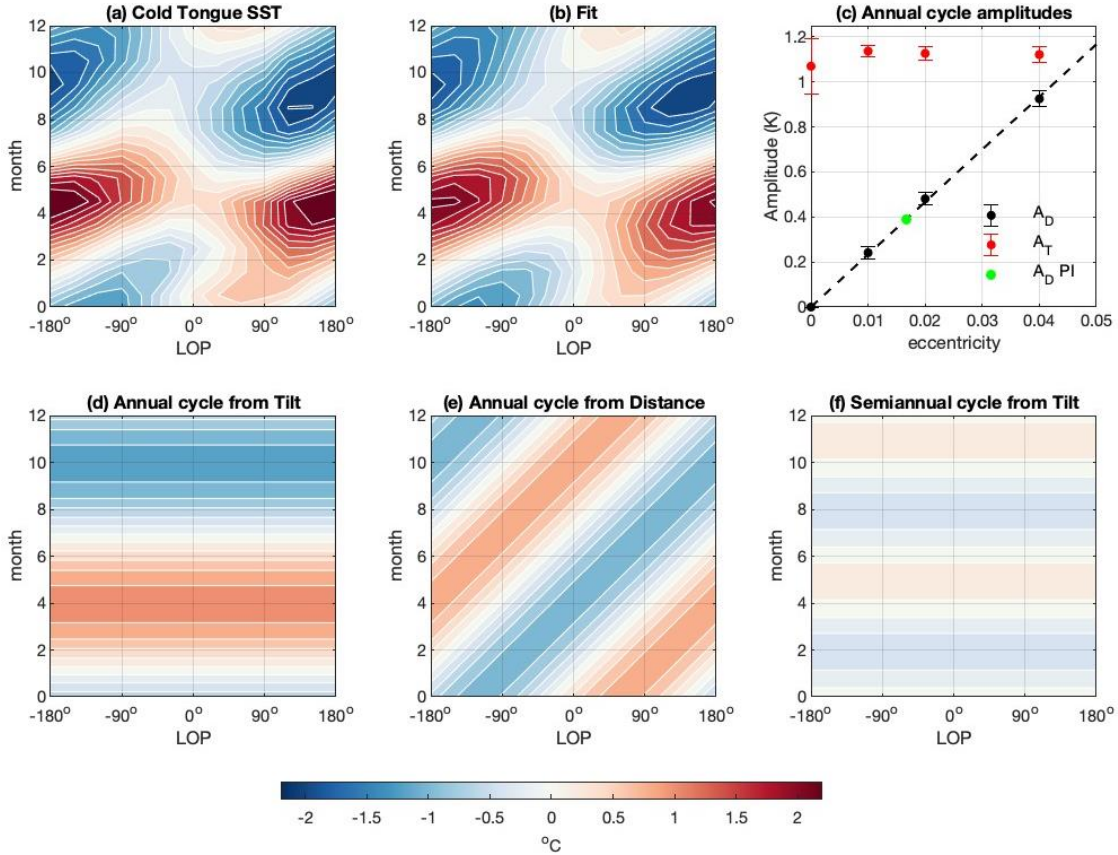


Figure 5. Change in the cold tongue annual cycle with the longitude of perihelion and decomposition into contributions from the annual cycle from tilt, annual cycle from distance, and semiannual cycle from tilt as reported in Chiang et al. (2022). (a) Cold tongue SST (averaged over 6° S– 6° N, 140 – 90° W) seasonal cycle for $e = 0.04$ with varying longitude of perihelion. The annual mean is removed from each annual cycle before plotting. **(b)** Least-square surface fit of the data in (a), using equation (1) (see section 6 for details of the calculation). **(c)**, Fitted coefficients of the distance effect amplitude (A_D , black symbols) and the least-square linear fit to the data forced through the intercept (dashed line). The bars indicate the 95% confidence bounds for each A_D fit. For comparison, the fitted coefficients of the tilt effect amplitude (A_T) are shown in red. The green dot indicates the distance effect amplitude for eccentricity at pre-industrial (PI) level ($e = 0.0167$). **(d)–(f)** Contributions of the fit in (b) from tilt effect annual cycle, distance effect annual cycle, and tilt effect semiannual cycle, respectively. Note that the month axis for used in (a), (b), (d), (e), and (f) is such that 0 is the start of the year and 12 is the end; mid-January is thus 0.5. Reproduced from Chiang et al. (2022), Figure 3.

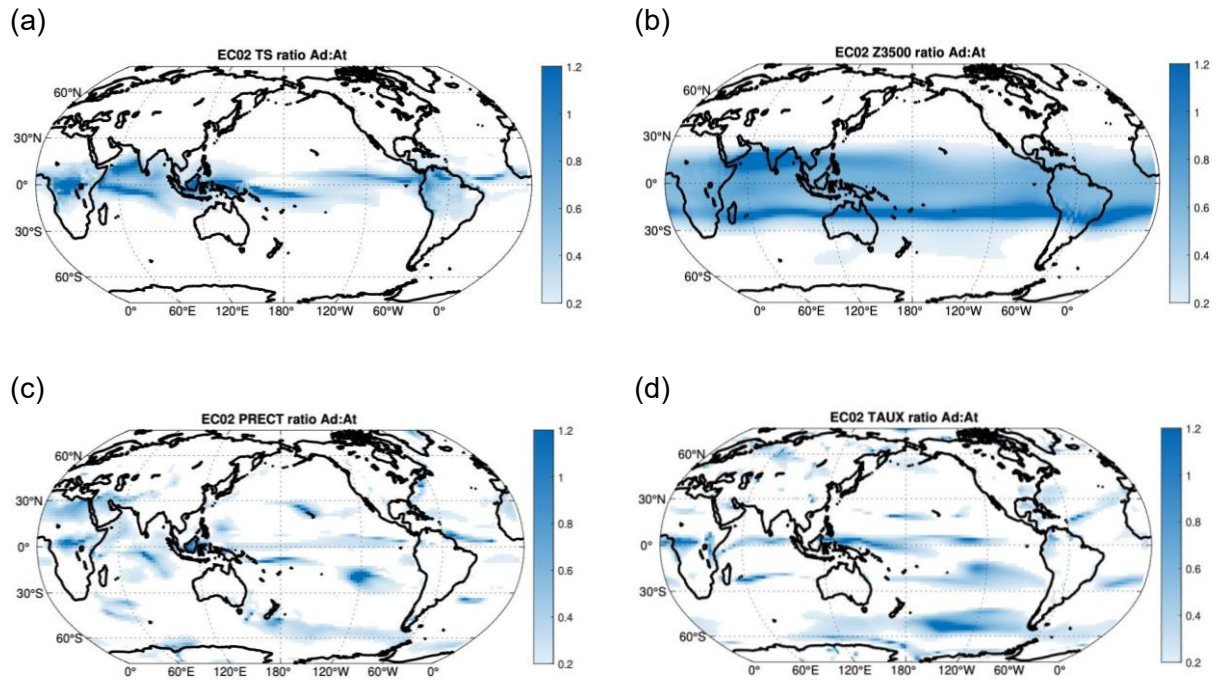


Figure 6. The relative contributions of distance and tilt to the annual cycle for various fields. The ratio of distance effect amplitude to tilt effect amplitude for (a) surface temperature, (b) 500mb geopotential height, (c) precipitation, and (d) zonal wind stress. The amplitudes are calculated by fitting equation 1 to each gridpoint, using the CESM LOP runs of Chiang et al. (2022) with $e = 0.02$. We use the $e = 0.02$ simulation here as it is close to the present-day value of $e \sim 0.017$. See section 6 for details of the calculation. Areas with no shading have ratios less than 20%; deep blue shading indicates that the distance effect amplitude is comparable or larger than the tilt effect amplitude.

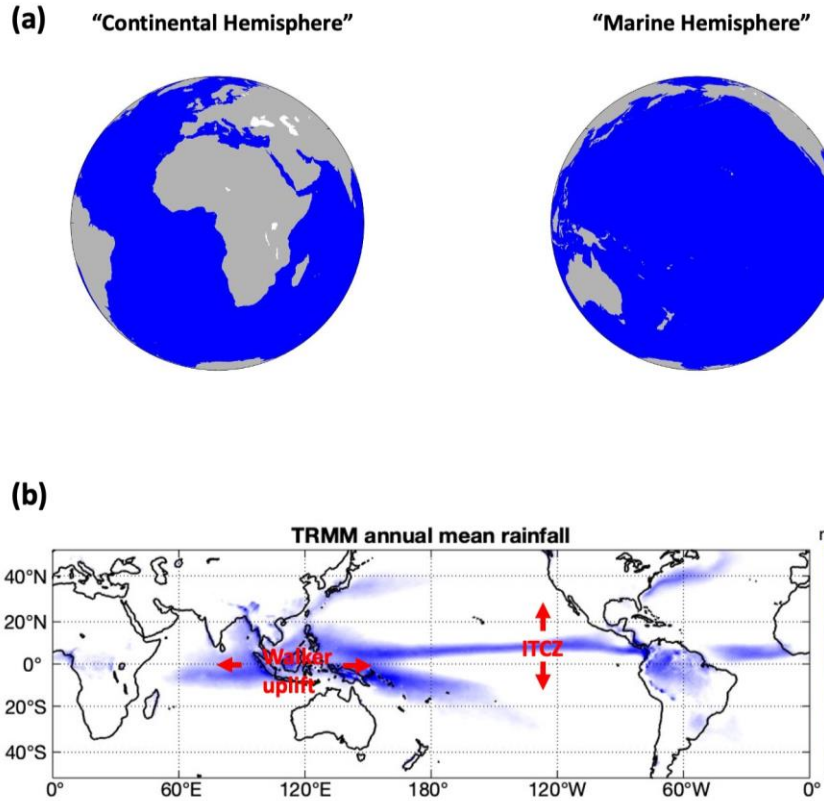


Figure 7. (a) Earth's continental distribution has a longitudinal asymmetry: the 'Marine' hemisphere centered over the Pacific is mostly ocean, whereas the opposing 'Continental' hemisphere centered over Africa is largely land. Insolation variations due to the distance effect act on the thermal difference between these hemispheres to produce the zonal wavenumber 1 seasonal response. (b) One consequence of the zonal interhemispheric seasonal response to the distance effect is an east-west seasonal migration of the Walker uplift region. It is the distance-effect analog of the north-south ITCZ migration from the tilt effect. The blue shading indicates the annual mean rainfall climatology (1998-2018) from the Tropical Rainfall Measuring Mission 3B43 dataset (Huffman et al. 2007).

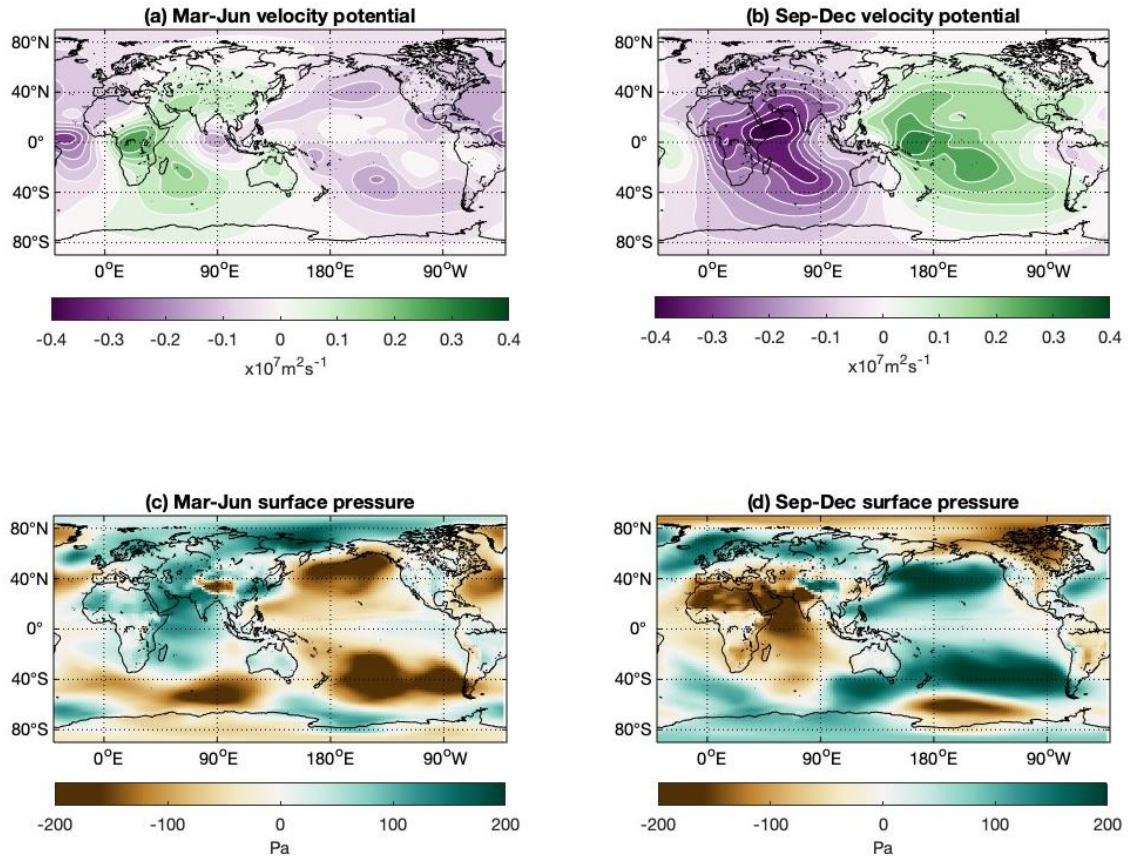


Figure 8. Zonal wavenumber 1 response to the distance-effect annual cycle. The difference between the distance-only run and zero annual forcing run (former minus latter) of Chiang et al. (2022) for **(a)** 200mb velocity potential averaged over March–June (following aphelion), and **(b)** September–December (following perihelion). The velocity potential change shows a predominantly zonal wavenumber 1 pattern with the nodal point over the Maritime continent, reversing in sign between March–June and September–December. **(c) and (d):** same as (a) and (b) respectively, but for surface pressure. The surface pressure change exhibits a see-saw in atmospheric mass between Africa/Indian ocean and the Pacific, again with the nodal point at the Maritime continent. Figure adapted from Chiang et al. (2022), Extended Data Figure 8.